Experimental and Theoretical Analysis of Hydrogen Bonding in Two-Dimensional Chiral 4',4''''-(1,4-Phenylene)bis(2,2':6',2 -terpyridine) Self-Assembled Nanoarchitecture

Manuela Mura, Fabien Silly

THE JOURNAL OF PHYSICAL CHEMISTRY C

Article

pubs.acs.org/JPCC

Experimental and Theoretical Analysis of Hydrogen Bonding in Two-Dimensional Chiral 4′,4‴′-(1,4-Phenylene)bis(2,2′:6′,2″-terpyridine) Self-Assembled Nanoarchitecture

Manuela Mura*,† and Fabien Silly*,‡

†Computational Physics Group, School of Mathematics and Physics, University of Lincoln, Brayford Pool, Lincoln LN6 7TS, U.K.

‡CEA, IRAMIS, SPEC, TITANS, CNRS, Université Paris-Saclay, F-91191 Gif sur Yvette, France

ABSTRACT: The two-dimensional self-assembly of 4′,4‴′-(1,4-phenylene)bis(2,2′:6′,2″-terpyridine) molecules is experimentally and theoretically investigated. Scanning tunneling microscopy (STM) shows that this molecular building block forms a compact chiral supramolecular network on graphite at the 1-octanol/graphite interface. The molecules adopt a side-by-side arrangement inside the organic domains. In contrast, the molecules are arranged perpendicularly at the domain boundary. Detailed theoretical analysis based on the density functional theory (DFT) shows that these arrangements are stabilized by double and single hydrogen bonds between pyridine groups. Only the molecular peripheral pyridine groups are involved in the hydrogen bonds stabilizing the long-range ordered molecular nanoarchitectures.

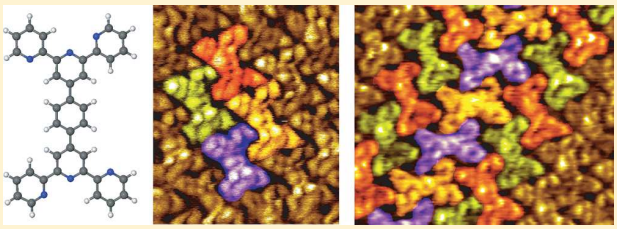

INTRODUCTION

Engineering novel organic nanoarchitectures through bottom-up strategy and molecular self-assembly[1−16] is attracting increasing interest over the past decade. Predicting and controlling self-assembly is a prerequisite to fabricate well-defined nanoarchitectures with specific local electronic properties.[17−19] Hydrogen bonding is an appealing intermolecular interaction to govern molecular self-assembly due to the high selectivity and high directionality of this bond.[20−27] Imide and carboxylic groups are functional units that can drive molecular self-assembly through the formation of double (N−H···O) or (O−H···O) hydrogen bonds, respectively.[28−30] The pyridine group is an interesting alternative to these substituents because of its flexibility. This group is not only expected to drive molecular self-assembly through the formation of double hydrogen bonds (C−H···N) between neighboring molecules, but the N atom can be located in different position of the benzene ring. The flexibility of this group opens new opportunities to engineer new architectures. Specific pyridine-based molecular building blocks have been recently synthesized[31,32] for application in the fields of supramolecular chemistry and materials science.[31] Hydrogen-bonded two-dimensional nanoarchitectures have been engineered using pyridine-based molecular building blocks.[33,34] The conformation of terpyridine compounds can change in organic nanoarchitectures according to Wang et al.[35] Perypherical pyridine groups can adopt a *trans* or *cis* conformation to confer stability to the molecular self-assembly. However, the strength of molecular bonds has not yet been assessed in terpyridine-compound self-assembly.

In this paper, we investigate the self-assembly of 4′,4‴′-(1,4-phenylene)bis(2,2′:6′,2″-terpyridine) molecules at the 1-octanol/graphite interface. Scanning tunneling microscopy (STM) reveals that the molecules self-assembled into a two-dimensional close-packed chiral nanoarchitecture. Molecules are arranged side-by-side inside the molecular domain whereas molecular are arranged perpendicularly at the domain boundary. Density functional theory (DFT) modeling reveals that this structures is stabilized by double and single hydrogen bonds between pyridine groups.

EXPERIMENTAL AND THEORETICAL METHODS

Solutions of 4′,4‴′-(1,4-phenylene)bis(2,2′:6′,2″-terpyridine) in 1-octanol (99%, Acros) were prepared. A droplet of this solution was then deposited on a graphite substrate. STM imaging of the samples was performed at the liquid/solid interface[36] using a Pico-SPM (Molecular Imaging, Agilent Technology) scanning tunneling microscope. Cut Pt/Ir tips were used to obtain constant current images at room temperature with a bias voltage applied to the sample. STM images were processed and analyzed using the application FabViewer.[37]

To model the molecular arrangement of the calculations 4′,4‴′-(1,4-phenylene)bis(2,2′:6′,2″-terpyridine) molecules simulations were performed using the *ab initio* SIESTA package.[38] SIESTA is based on the localized numerical orbital basis set, periodic boundary conditions, and the first-principles scalar-relativistic norm-conserving Troullier−Martins[39] pseudopotential factorized in the Kleinman−Bylander[40] form. We

Received: July 26, 2015
Revised: September 25, 2015
Published: October 8, 2015

DOI: 10.1021/acs.jpcc.5b07231
J. Phys. Chem. C 2015, 119, 27125−27130

used Perdew, Becke, and Ernzerhof (PBE)[41] generalized gradient approximation for the exchange and correlation, which was found previously to be adequate in representing hydrogen bonding between DNA base molecules.[42] In each calculation, atomic relaxation was performed until forces on atoms were less than 0.01 eV/Å in the cases of dimers and 0.03 eV/Å in the cases of monolayers. The effect of the vdW forces in the assembly of molecules on the surface has been considered thanks to the vdW-DF *ab initio* method.[43−45] The energetics of each gas-phase monolayer, calculated using SIESTA, is characterized by its stabilization energy, which is composed of two components: the interaction and deformation energies. If the former characterizes the strength of intermolecular interaction (it is negative), the latter shows the energy penalty due to inevitable deformation of molecules in the final structure (and is positive). The calculated energies include the basis set superposition error (BSSE) correction[46] due to the localized basis set used. To analyze bonding in the relaxed structures, the electron density difference (between the total density and that of all individual molecules in the geometry of the combined system) was found to be especially useful because the hydrogen bonding is known to be well characterized by the "kebab" structure associated with alternating regions of excess and depletion of the electron density along the donor−hydrogen−acceptor line of atoms.[42]

RESULTS AND DISCUSSION

The chemical structure of the 4′,4‴′-(1,4-phenylene)bis-(2,2′:6′,2″-terpyridine) molecule is presented in Figure 1. This 2-fold symmetry molecule is a H-shaped molecule. Its skeleton consists of a central benzene ring connected to two peripheral terpyridine groups.

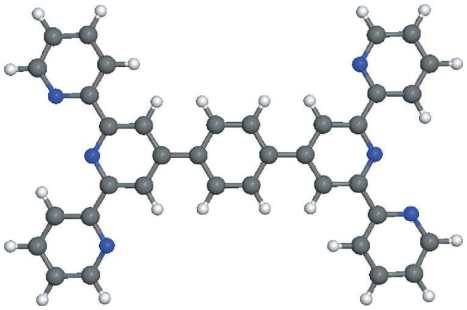

Figure 1. 4′,4‴′-(1,4-Phenylene)bis(2,2′:6′,2″-terpyridine) molecule ($C_{36}H_{24}N_6$). Carbon atoms are gray, hydrogen atoms are white, and nitrogen atoms are blue, respectively.

Figure 2a, the large scale STM image, reveals that 4′,4‴′-(1,4-phenylene)bis(2,2′:6′,2″-terpyridine) molecules self-assemble into large close-packed nanoarchitectures at the 1-octanol/graphite interface. The molecules are entirely covering the graphite surface. This molecular arrangement is chiral and is stable during STM imaging. The two enantiomeric structures are visible in the high resolution STM images presented in Figure 2b,c. Intramolecular features corresponding to the integrated density of states of the molecule appear distinctly in the high resolution STM images, Figure 2b,c. The molecules forming the chiral network unit cells have been colored in yellow, red, blue, and green as a guide for the eyes. Neighboring molecules are arranged parallel to each other. The model of this self-assembled nanoarchitecture is presented in Figure 4a. The

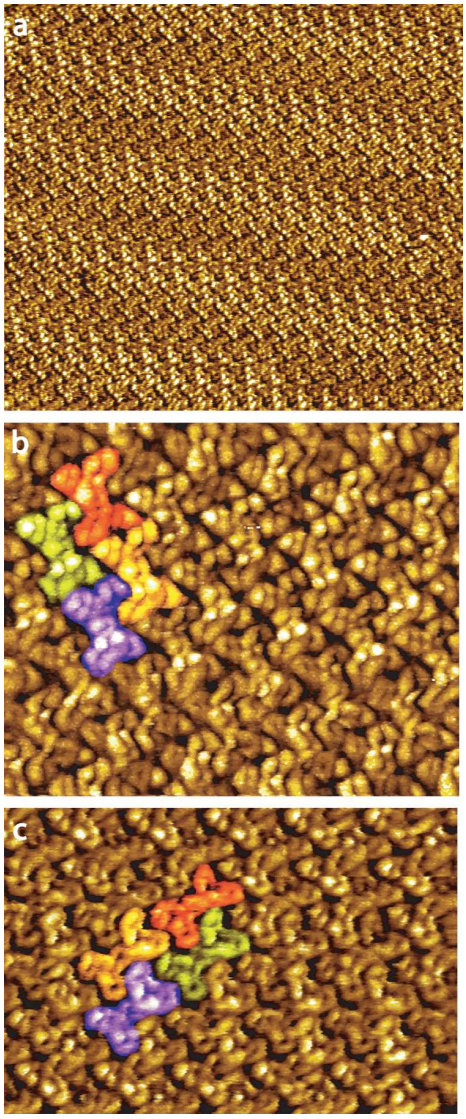

Figure 2. (a) Large scale STM image of 4′,4‴′-(1,4-phenylene)bis-(2,2′:6′,2″-terpyridine) chiral nanoarchitecture on graphite, 30 × 26 nm^2; V_s = 0.5 V, I_t = 180 pA. The two enantiomeric domains are presented in the high-resolution STM images: (b) 9 × 8 nm^2, V_s = 0.5 V, I_t = 180 pA; (c) 9 × 7 nm^2, V_s = 0.5 V, I_t = 180 pA. Molecules comprising the unit cell are in red, green, blue, and yellow in (b) and (c).

network unit cell of this close-packed structure is a parallelogram with 2.0 ± 0.2 and 1.4 ± 0.2 nm unit cell constants (A_1, A_2) and an angle θ of 67 ± 3° between the axes, Table 1. The lattice vectors (A_1, A_2) are represented by purple arrows in Figure 4a.

An STM image of the domain boundary is presented in Figure 3. The molecules at the edge of the domains have been colored in red and green, as a guide for the eyes. The molecules of neighboring domains are aligned (red, green molecules). The two domains are separated by a molecular row (molecules colored in yellow and blue). The molecules of this row are parallel to each other, but they are rotated by 80° with respect to the molecules of the domains. The molecules of the side-by-side arrangement are epitaxially oriented on the graphite surface. The perpendicular molecules are in contrast aligned in

DOI: 10.1021/acs.jpcc.5b07231
J. Phys. Chem. C 2015, 119, 27125−27130

Table 1. Unit Cell Parameters: Lengths of the Two Lattice Vectors (A_1, A_2) and the Angle θ between Them for the 4′,4‴′-(1,4-Phenylene)bis(2,2′:6′,2″-terpyridine) Nanoarchitecture[a]

phase	parallel		perpendicular	
technique:	STM	DFT	STM	DFT
A_1 (Å)	20	18.8	34	31.5
A_2 (Å)	14	13.4	14	12.9
θ (deg)	67	65	85	89
τ (deg)	0	0	77	77

[a]The difference in the orientations of the two molecules within the cell is shown by the angle τ.

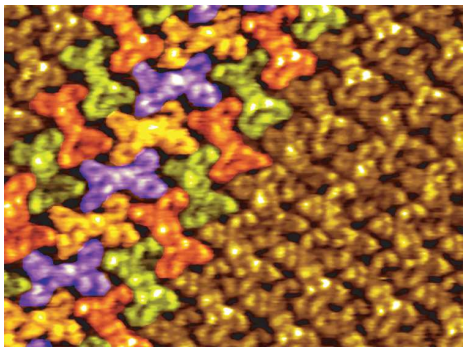

Figure 3. STM image of the 4′,4‴′-(1,4-phenylene)bis(2,2′:6′,2″-terpyridine) nanoarchitecture domain boundary, 10 × 8 nm^2; V_s = 0.5 V, I_t = 180 pA. Molecules of the domain edge are in red and green. Molecules separating the neighboring domains are in yellow and blue.

another crystalline direction of the graphite surface. The network unit cell at the domain boundary is represented by a purple dashed line in the model shown in Figure 5a. The boundary unit cell is a parallelogram with 3.4 ± 0.3 and 1.4 ± 0.3 nm unit cell constants and an angle θ of 85 ± 4° between the axes, Table 1. The lattice vectors (A_1, A_2) are represented by purple arrows in Figure 5a.

Hoster et al. previously investigated the hydrogen-binging in bis(terpyridine) derivative arrangements.[47] They theoretically estimated intermolecular interaction by modeling the interaction of free benzene and pyridine rings. Their calculations show that N···H interaction energy is drastically stronger than H···H interaction. Their model, however, does not take into account the whole molecular structure. It was also assumed that the molecules were adopting a planar configuration in these calculations.

In our calculations, the whole molecular structure is modeled and the possibility that molecular structure can adopt different configurations is also taken into account. For the parallel and perpendicular networks, two unit cells were considered. The unit cells are composed of two and four molecules, respectively. The two geometries reveal a similar stabilization energy and energy per molecule for the two nanoarchitectures (Table 2). The perpendicular arrangement of molecular dimers is slightly more stable than the parallel configuration when two molecules are considered. In contrast, the perpendicular arrangement appears to be less stable when four molecules in the unit cell are considered (Table 2). The density of the perpendicular arrangement (0.47 mol/nm^2) is slightly larger than the one of the parallel arrangement (0.44 mol/nm^2). In fact, the perpendicular configuration of tetramers becomes less stable because it induces a distortion of molecular conformation in the unit cell. The molecular peripherical pyridine groups are rotating with respect to the molecular plane; i.e., the terpyridine groups are then not flat. This rotation weakens the hydrogen bond between neighboring molecules and increases the energy of the molecular arrangement.

The calculations reveal that the unit cell (containing one molecule) of the parallel arrangement is stabilized by two double H-bonds highlighted by dark blue circles in Figure 4c. In comparison, the monolayer based on the perpendicular tetramers (Figure 5c) contains two molecules per unit cell, which is stabilized by two double H-bond (dark blue circles) and two single H-bonds (light blue circles), Figure 5c. The gray circle highlights a charge rearrangement, which does not correspond to a H-bond. The unit cell of the parallel arrangement is therefore stabilized by a higher number of H-bonds per molecules than the unit cell of the perpendicular arrangement. However, calculations only reveal a small difference in energy between the two assemblies (Table 3), which indicates that the hydrogen bonds between neighboring molecules are stronger in the perpendicular tetramer than in the aligned tetramers when the monolayer is formed. The difference in strength between the two assembles can be observed in the "kebab" plot in Figures 4 and 5. In these plots, the alternating regions of depletion and excess of the density along the H-bonds characterize the strength of the bonding. The molecules are bonded to each other through two N···H−C bonds between their peripheral terpyridine groups in the parallel arrangement, Figure 4b. In contrast, the N atom of the molecular central terpyridine group is not involved in any H-

Table 2. Calculated Energies: Building Blocks and Calculated Energies of the 4′,4‴′-(1,4-Phenylene)bis(2,2′:6′,2″-terpyridine) Networks (PBE, BSSE, and Cohesion Energies, E_{coh})

Structure	Parallel		Perpendicular	
	Dimer	Tetramer	Dimer	Tetramer
Molecular block	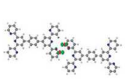		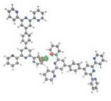	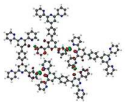
Energy (eV) (PBE)	-0.35	-0.87	-0.41	-0.63
BSSE Energy (eV)	0.04	0.2	0.04	0.2
E_{coh} (eV) per molecule	0.18	0.22	0.21	0.16

DOI: 10.1021/acs.jpcc.5b07231
J. Phys. Chem. C 2015, 119, 27125−27130

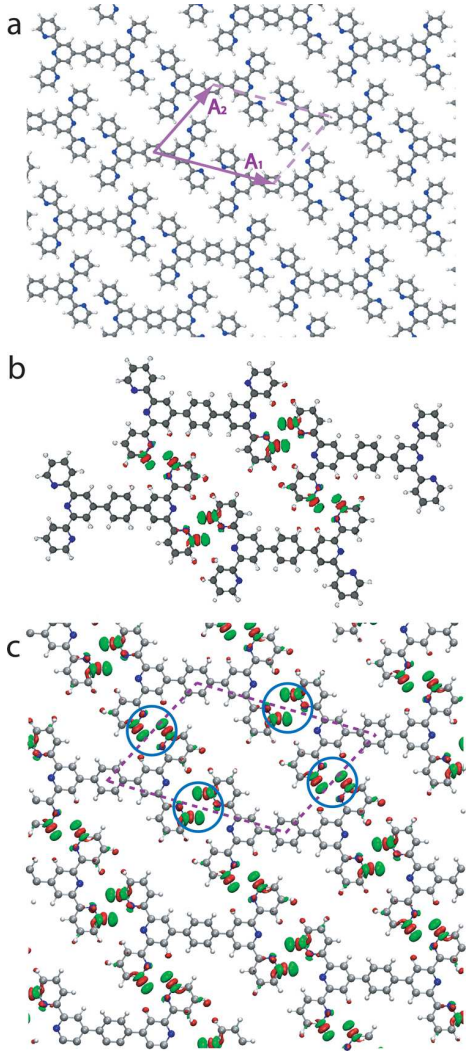

Figure 4. (a) Model of the 4′,4‴″-(1,4-phenylene)bis(2,2′:6′,2″-terpyridine) nanoarchitecture. The lattice vectors A_1 and A_2 are indicated by arrows, and the unit cell is indicated by a dashed box for convenience. (b) Geometries of the 4′,4‴″-(1,4-phenylene)bis-(2,2′:6′,2″-terpyridine) tetramer shown together with the electron density difference plots corresponding to ±0.005 Å^{-3}. The green surfaces correspond to the regions of positive electron density difference (excess) and the red areas correspond to the regions of negative electron density difference (depletion). (c) Electron density difference plot of the molecular network.

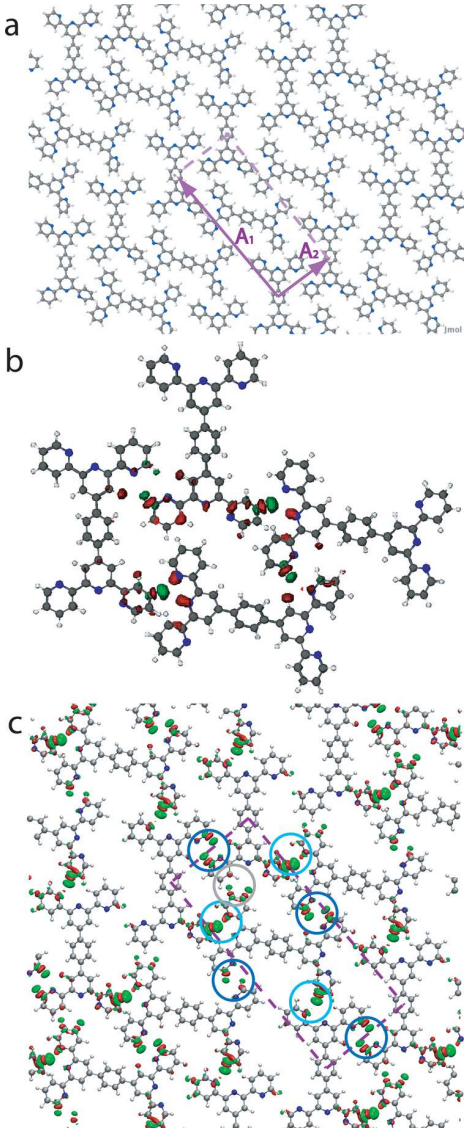

Figure 5. Geometries of the 4′,4‴″-(1,4-phenylene)bis(2,2′:6′,2″-terpyridine) tetramer shown together with the electron density difference plots corresponding to ±0.005 Å^{-3}. The green surfaces correspond to the regions of positive electron density difference (excess), and the red areas correspond to the regions of negative electron density difference (depletion). (c) Electron density difference plot of the molecular perpendicular arrangement.

bond. In comparison, the central pyridine group is forming a H-bond with the periperical pyridine group of a neighboring molecule in the perpendicular arrangement, when only four molecules are considered, Figure 5b. It should be noticed that the electrostatic plot shows an incomplete "kebab" in the proximity of the nitrogen atom of each terpyridine groups, which underlines the weakness of this bond. The calculations presented in Figure 5c reveal that the central pyridine group is not involved in H-bonding when the tetramer periodic images are chosen to interact between each other to mimic the monomer periodic structure experimentally observed in Figure 3.

The calculated gas-phase parallel and perpendicular configurations are in good agreement with experimental observations,

Table 3. Cohesion Energies: Number of Molecules per Unit Cell and Calculated Cohesion Energies E_{coh} per Molecule of the 4′,4‴″-(1,4-Phenylene)bis(2,2′:6′,2″-terpyridine) Network

structure	parallel	perpendicular
energy (eV) (PBE)	−1.16	−1.06
BSSE energy (eV)	0.28	0.30
E_{coh} (eV)	−0.29	−0.27

Table 1. The perpendicular configuration does, however, present some slight differences. These are probably induced by the molecular distortion, which leads to a noticeable nonplanar configuration. The presence of a surface is expected to reduce this effect and limit the variation of molecular

DOI: 10.1021/acs.jpcc.5b07231
J. Phys. Chem. C 2015, 119, 27125−27130

conformation in comparison with the gas-phase configuration. In contrast, the parallel arrangement is expected to be less influenced by the presence of the surface as the molecular distortion is smaller in this structure. In addition, these molecules appear to be aligned in a preferential direction of the graphite surface (epitaxial domains). This is not the case for the perpendicular molecules. The experimental stabilization energy of this perpendicular arrangement will therefore decrease and so be less favorable when compared with that of the parallel arrangement. This explains, therefore, why the perpendicular arrangement is only locally observed at the domain boundary in the STM images. It should be noticed that a Moiré pattern can be observed in the STM images for the parallel arrangement. This suggests some electronic coupling between the molecules and the substrate,[48] but this also reveals that there is no preferential adsorption site for the molecules along the graphite direction.

CONCLUSION

In this paper we investigated the two-dimensional self-assembly of 4′,4‴-(1,4-phenylene)bis(2,2′:6′,2″-terpyridine) on a graphite surface. Molecules adopt a side-by-side arrangement inside the monolayer but are arranged perpendicularly at the domain boundary. Experimental observations and calculations reveal that the molecule forms a close-packed structure stabilized by double and single hydrogen-bonds. Calculations show that the molecular conformation is less planar in the perpendicular molecular packing than in the molecular parallel packing. The flexibility of terpyridine groups open new opportunities to engineer new organic nanoarchitectures on surfaces.

AUTHOR INFORMATION

Corresponding Authors

*E-mail: mmura@lincoln.ac.uk. Phone: +44 (0)1522835866.
*E-mail: fabien.silly@cea.fr. Phone: +33(0)169088019. Fax: +33(0)169088446.

Notes

The authors declare no competing financial interest.

ACKNOWLEDGMENTS

The research leading to these results has received funding from the European Research Council under the European Union's Seventh Framework Programme (FP7/2007-2013)/ERC grant agreement no. 259297.

REFERENCES

(1) Shang, J.; Wang, Y.; Chen, M.; Dai, J.; Zhou, X.; Kuttner, J.; Hilt, G.; Shao, X.; Gottfried, J. M.; Wu, K. Assembling Molecular Sierpiński Triangle Fractals. *Nat. Chem.* **2015**, *7*, 389−393.
(2) Pawin, G.; Wong, K. L.; Kwon, K.-Y.; Bartels, L. A Homomolecular Porous Network at a Cu(111)Surface. *Science* **2006**, *313*, 961−962.
(3) Wu, R.; Yan, L.; Zhang, Y.; Ren, J.; Bao, D.; Zhang, H.; Wang, Y.; Du, S.; Huan, Q.; Gao, H.-J. Self-Assembled Patterns and Young's Modulus of Single-Layer Naphthalocyanine Molecules on Ag(111). *J. Phys. Chem. C* **2015**, *119*, 8208−8212.
(4) Wang, Q. H.; Hersam, M. C. Room-Temperature Molecular-Resolution Characterization of Self-Assembled Organic Monolayers on Epitaxial Graphene. *Nat. Chem.* **2009**, *1*, 206−211.
(5) Lu, J.; Yeo, P. S. E.; Zheng, Y.; Yang, Z.; Bao, Q.; Gan, C. K.; Loh, K. P. Using the Graphene Moiré Pattern for the Trapping of C_{60} and Homoepitaxy of Graphene. *ACS Nano* **2012**, *6*, 944−950.
(6) Maeda, H. Supramolecular Chemistry of Pyrrole-Based π-Conjugated Molecules. *Bull. Chem. Soc. Jpn.* **2013**, *86*, 1359−1399.
(7) Amrous, A.; Bocquet, F.; Nony, L.; Para, F.; Loppacher, C.; Lamare, S.; Palmino, F.; Cherioux, F.; Gao, D. Z.; Canova, F. F.; et al. Molecular Design and Control Over the Morphology of Self-Assembled Films on Ionic Substrates. *Adv. Mater. Interfaces* **2014**, *1*, 1400414.
(8) Uemura, S.; Aono, M.; Sakata, K.; Komatsu, T.; Kunitake, M. Thermodynamic Control of 2D Bicomponent Porous Networks of Melamine and Melem: Diverse Hydrogen-Bonded Networks. *J. Phys. Chem. C* **2013**, *117*, 24815−24821.
(9) Kikkawa, Y.; Ishitsuka, M.; Kashiwada, A.; Tsuzuki, S.; Hiratani, K. Bicomponent Blend-Directed Amplification of the Alkyl Chain Effect on the 2D Structures. *Chem. Commun.* **2014**, *50*, 13146−13149.
(10) Li, M.; Zeng, Q.; Wang, C. Self-Assembled Supramolecular Networks at Interfaces: Molecular Immobilization and Recognition Using Nanoporous Templates. *Sci. China: Phys., Mech. Astron.* **2011**, *54*, 1739−1748.
(11) Liang, H.; He, Y.; Ye, Y.; Xu, X.; Cheng, F.; Sun, W.; Shao, X.; Wang, Y.; Li, J.; Wu, K. Two-Dimensional Molecular Porous Networks Constructed by Surface Assembling. *Coord. Chem. Rev.* **2009**, *253*, 2959−2979.
(12) Otsuki, J. STM Studies on Porphyrins. *Coord. Chem. Rev.* **2010**, *254*, 2311−2341.
(13) Rosei, F.; Schunack, M.; Naitoh, Y.; Jiang, P.; Gourdon, A.; Laegsgaard, E.; Stensgaard, I.; Joachim, C.; Besenbacher, F. Properties of Large Organic Molecules on Metal Surfaces. *Prog. Surf. Sci.* **2003**, *71*, 95−146.
(14) Roy, B.; Bairi, P.; Nandi, A. K. Supramolecular Assembly of Melamine and its Derivatives: Nanostructures to Functional Materials. *RSC Adv.* **2014**, *4*, 1708−1734.
(15) Yagai, S. Supramolecularly Engineered Functional π-Assemblies Based on Complementary Hydrogen-Bonding Interactions. *Bull. Chem. Soc. Jpn.* **2015**, *88*, 28−58.
(16) Yang, Y.; Wang, C. Hierarchical Construction of Self-Assembled Low-Dimensional Molecular Architectures Observed by Using Scanning Tunneling Microscopy. *Chem. Soc. Rev.* **2009**, *38*, 2576.
(17) Hieulle, J.; Silly, F. Localized Intermolecular Electronic Coupling in Two-Dimensional Self-Assembled 3,4,9,10-perylenetetracarboxylic Diimide Nanoarchitectures. *J. Mater. Chem. C* **2013**, *1*, 4536−4539.
(18) Sedona, F.; Marino, M. D.; Forrer, D.; Vittadini, A.; Casarin, M.; Cossaro, A.; Floreano, L.; Verdini, A.; Sambi, M. Tuning the catalytic activity of Ag(110)-supported Fe phthalocyanine in the oxygen reduction reaction. *Nat. Mater.* **2012**, *11*, 970−977.
(19) Gusev, A. O.; Taleb, A.; Silly, F.; Charra, F.; Pileni, M.-P. Inhomogeneous Photon Emission Properties of Self-Assembled Metallic Nanocrystals. *Adv. Mater.* **2000**, *12*, 1583−1587.
(20) Yagai, S.; Goto, Y.; Lin, X.; Karatsu, T.; Kitamura, A.; Kuzuhara, D.; Yamada, H.; Kikkawa, Y.; Saeki, A.; Seki, S. Self-Organization of Hydrogen-Bonding Naphthalene Chromophores into J-type Nanorings and H-type Nanorods: Impact of Regioisomerism. *Angew. Chem., Int. Ed.* **2012**, *51*, 6643−6647.
(21) Barth, J. V. Molecular Architectonic on Metal Surfaces. *Annu. Rev. Phys. Chem.* **2007**, *58*, 375−407.
(22) Mura, M.; Sun, X.; Silly, F.; Jonkman, H. T.; Briggs, G. A. D.; Castell, M. R.; Kantorovich, L. N. Experimental and Theoretical Analysis of H-Bonded Supramolecular Assemblies of PTCDA Molecules. *Phys. Rev. B: Condens. Matter Mater. Phys.* **2010**, *81*, 195412.
(23) Yagai, S.; Iwai, K.; Yamauchi, M.; Karatsu, T.; Kitamura, A.; Uemura, S.; Morimoto, M.; Wang, H.; Würthner, F. Photocontrol Over Self-Assembled Nanostructures of π-π Stacked Dyes Supported by the Parallel Conformer of Diarylethene. *Angew. Chem., Int. Ed.* **2014**, *53*, 2602−2606.
(24) De Feyter, S.; De Schryver, F. C. Two-Dimensional Supramolecular Self-Assembly Probed by Scanning Tunneling Microscopy. *Chem. Soc. Rev.* **2003**, *32*, 139−150.
(25) Sun, X.; Jonkman, H. T.; Silly, F. Tailoring Two-Dimensional PTCDA-melamine Self-Assembled Architectures at Room Temperature by Tuning Molecular Ratio. *Nanotechnology* **2010**, *21*, 165602.

DOI: 10.1021/acs.jpcc.5b07231
J. Phys. Chem. C 2015, 119, 27125−27130

(26) Bonifazi, D.; Mohnani, S.; Llanes-Pallas, A. Supramolecular Chemistry at Interfaces: Molecular Recognition on Nanopatterned Porous Surfaces. *Chem. - Eur. J.* **2009**, *15*, 7004−7025.
(27) Mura, M.; Silly, F.; Burlakov, V.; Castell, M. R.; Briggs, G. A. D.; Kantorovich, L. N. Formation Mechanism for a Hybrid Supramolecular Network Involving Cooperative Interactions. *Phys. Rev. Lett.* **2012**, *108*, 176103.
(28) Hu, F.-Y.; Zhang, X.-M.; Wang, X.-C.; Wang, S.; Wang, H.-Q.; Duan, W.-B.; Zeng, Q.-D.; Wang, C. In Situ STM Investigation of Two-Dimensional Chiral Assemblies through Schiff-Base Condensation at a Liquid/Solid Interface. *ACS Appl. Mater. Interfaces* **2013**, *5*, 1583−1587.
(29) Suh, M. P.; Cheon, Y. E.; Lee, E. Y. Syntheses and Functions of Porous Metallosupramolecular Networks. *Coord. Chem. Rev.* **2008**, *252*, 1007−1026.
(30) Zhang, X.; Zeng, Q.; Wang, C. Molecular Templates and Nano-Reactors: Two-Dimensional Hydrogen Bonded Supramolecular Networks on Solid/Liquid Interfaces. *RSC Adv.* **2013**, *3*, 11351−11366.
(31) Wild, A.; Winter, A.; Schlütter, F.; Schubert, U. S. Advances in the Field of π-Conjugated 2,2′:6′,2″-terpyridines. *Chem. Soc. Rev.* **2011**, *40*, 1459−1511.
(32) Earmme, T.; Jenekhe, S. A. Solution-Processed, Alkali Metal-Salt-Doped, Electron-Transport Layers for High-Performance Phosphorescent Organic Light-Emitting Diodes. *Adv. Funct. Mater.* **2012**, *22*, 5126−5136.
(33) Roos, M.; Künzel, D.; Uhl, B.; Huang, H.-H.; Brandao Alves, O.; Hoster, H. E.; Gross, A.; Behm, R. J. Hierarchical Interactions and Their Influence upon the Adsorption of Organic Molecules on a Graphene Film. *J. Am. Chem. Soc.* **2011**, *133*, 9208−9211.
(34) Meier, C.; Landfester, K.; Ziener, U. Adsorbate-Substrate-Mediated Growth of Oligopyridine Monolayers at the Solid/Liquid Interface. *J. Phys. Chem. C* **2009**, *113*, 1507−1514.
(35) Wang, S.; Zhao, F.; Luo, S.; Geng, Y.; Zeng, Q.; Wang, C. Solvent-Induced Variable Conformation of Bis(terpyridine) Derivatives During Supramolecular Self-Assembly at Liquid/HOPG Interfaces. *Phys. Chem. Chem. Phys.* **2015**, *17*, 12350−12355.
(36) Silly, F. Selecting Two-Dimensional Halogen-Halogen Bonded Self-Assembled 1,3,5-Tris(4-iodophenyl)benzene Porous Nanoarchitectures at the Solid-Liquid Interface. *J. Phys. Chem. C* **2013**, *117*, 20244−20249.
(37) Silly, F. A Robust Method For Processing Scanning Probe Microscopy Images and Determining Nanoobject Position and Dimensions. *J. Microsc.* **2009**, *236*, 211−218.
(38) Sánchez-Portal, D.; Ordejón, P.; Artacho, E.; Soler, J. M. Density-Functional Method for Very Large Systems with LCAO Basis Sets. *Int. J. Quantum Chem.* **1997**, *65*, 453−461.
(39) Troullier, N.; Martins, J. L. Efficient Pseudopotentials for Plane-Wave Calculations. *Phys. Rev. B: Condens. Matter Mater. Phys.* **1991**, *43*, 1993.
(40) Kleinman, L. Relativistic Norm-Conserving Pseudopotential. *Phys. Rev. B: Condens. Matter Mater. Phys.* **1980**, *21*, 2630.
(41) Perdew, J. P.; Burke, K.; Ernzerhof, M. Generalized Gradient Approximation Made Simple. *Phys. Rev. Lett.* **1996**, *77*, 3865−3868.
(42) Kelly, R. E. A.; Lee, Y. J.; Kantorovich, L. N. Homopairing Possibilities of the DNA Bases Cytosine and Guanine: An ab Initio DFT Study. *J. Phys. Chem. B* **2005**, *109*, 22045−22052.
(43) Dion, M.; Rydberg, H.; Schröder, E.; Langreth, D. C.; Lundqvist, B. I. Van der Waals Density Functional for General Geometries. *Phys. Rev. Lett.* **2004**, *92*, 246401.
(44) Thonhauser, T.; Cooper, V. R.; Li, S.; Puzder, A.; Hyldgaard, P.; Langreth, D. C. Van der Waals Density Functional: Self-Consistent Potential and the Nature of the van der Waals Bond. *Phys. Rev. B: Condens. Matter Mater. Phys.* **2007**, *76*, 125112.
(45) Cooper, V. R.; Thonhauser, T.; Puzder, A.; Schröder, E.; Lundqvist, B. I.; Langreth, D. C. Stacking Interactions and the Twist of DNA. *J. Am. Chem. Soc.* **2008**, *130*, 1304−1308.
(46) Boys, S. F.; Bernardi, F. The Calculation of Small Molecular Interactions by the Differences of Separate Total Energies. Some Procedures with Reduced Errors. *Mol. Phys.* **1970**, *19*, 553−566.
(47) Hoster, H. E.; Roos, M.; Breitruck, A.; Meier, C.; Tonigold, K.; Waldmann, T.; Ziener, U.; Landfester, K.; Behm, R. J. Structure Formation in Bis(terpyridine) Derivative Adlayers:Molecule-Substrate versus Molecule-Molecule Interactions. *Langmuir* **2007**, *23*, 11570−11579.
(48) Silly, F. Moiré Pattern Induced by the Electronic Coupling Between 1-Octanol Self-Assembled Monolayers and Graphite Surface. *Nanotechnology* **2012**, *23*, 225603.

DOI: 10.1021/acs.jpcc.5b07231
J. Phys. Chem. C 2015, 119, 27125−27130